



## Thermal stability, thermokinetic, and decomposition mechanism of copper(II) triazole-3-thiones complexes

S.A.Ibrahim, S.A.El-Gyar, A.Abd El-Sameh\*, M.A.El-Gahami

Chemistry Department, Faculty of Science, Assiut University, Assiut 71516, (EGYPT)

E-mail : drlahmed@yahoo.com

Received: 27<sup>th</sup> June, 2009 ; Accepted: 7<sup>th</sup> July 2009

### ABSTRACT

The thermal decomposition study of copper(II) complexes [a series of copper(II) complexes with 4-amino-5-benzyl-4H-1,2,4-triazole-3-thione (ABT), 5-benzyl-4-(benzylideneamino)-4H-1,2,4-triazole-3-thione (BBT), 5-benzyl-4-[(2-hydroxybenzylidene)amino]-4H-1,2,4-triazole-3-thione (HBHT) and 5-benzyl-4-[(4-methoxybenzylidene)amino]-4H-1,2,4-triazole-3-thione (BMT)] was monitored by TG, DTG and DTA analysis in dynamic atmosphere of nitrogen. TG, DTG and DTA studies confirmed the chemical formulations of these complexes and showed that their thermal degradation take place in two to four steps depending on the type of ligand present. The kinetic parameters were determined from the thermal decomposition data using the graphical methods of Coats-Redfern and Horowitz-Metzger. Thermodynamic parameters were calculated using standard relations. Negative values of the entropy indicate a more ordered activated state that may be possible through the chemisorption of oxygen and other decomposition products. In most cases the values of the activation energy for the second decomposition stage were found to be higher than that of the first stage, this may be attributed to the structural rigidity of the ligands. The decomposition stability order of the complexes depends on the structural feature of ligand, copper(II) complex containing the ABT ligand being the most stable one. The activation energies of the thermal degradation steps lie in the range 9.83-70.86 kJmol<sup>-1</sup>.

© 2009 Trade Science Inc. - INDIA

### KEYWORDS

Thermal stability;  
Kinetic parameters;  
Thermodynamic parameters;  
Triaazole-3-thiones complexes.

### 1. INTRODUCTION

Triazole-3-thiones and their complexes have been reported to be biologically versatile compounds having bactericidal properties. Amine and thione-substituted triazoles have been studied as anti-inflammatory and antimicrobial agents<sup>[1,2]</sup>. As such, they are part of the larger family of sulfur and nitrogen containing organic compounds which display a broad range of biological activity, finding applications as antitumor, antibacterial,

antifungal and antiviral agents<sup>[3-5]</sup>. The chemistry of transition metal complexes with heterocyclic thiones continues to be of interest, because of their striking structural features as well as their biological importance<sup>[6-8]</sup>. However, information on complexes derived from substituted 1,2,4-triazoles is scanty<sup>[9-11]</sup>.

To the best of our knowledge very little work has been done on the thermal behaviour of triazole-3-thiones-metal complexes of transition elements<sup>[12-23]</sup>. Hence the present paper reports the thermal analysis studies of some

## Full Paper

copper(II) triazole-3-thiones complexes. The associated thermal decomposition mechanisms are proposed. The kinetic parameters: order of the decomposition reaction ( $n$ ), correlation coefficient ( $r$ ), activation energy ( $E^\ddagger$ ) and pre-exponential factor (collision factor) ( $Z$ ) were determined from the thermal decomposition data using the graphical methods of Coats-Redfern and Horowitz-Metzger<sup>[24,25]</sup>. Thermodynamic parameters: entropy ( $\Delta S^\ddagger$ ), enthalpy ( $\Delta H^\ddagger$ ) and Gibbs free energy ( $\Delta G^\ddagger$ ) of activation, were calculated using a standard relations<sup>[26]</sup>. Structural representation of the ligands and abbreviations are given in Figure 1.

## 2. EXPERIMENTAL

All chemicals used in the preparative work were of A.R. or equivalent grade, they include the following: carbon disulfide, potassium hydroxide, absolute ethanol, phenylacetic acid, hydrazine, diethyl ether, hydrochloric acid, benzylaldehyde, salicylaldehyde, p-methoxybenzylaldehyde and piperidine. The metal salt  $\text{CuCl}_2 \cdot 2\text{H}_2\text{O}$  used was of general reagent grade.

### 2.1 Ligand preparation ABT, BBT, HBHT, BMT

They were prepared following the literature procedure<sup>[27-30]</sup>.

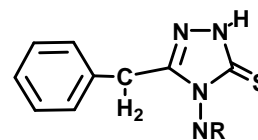
**ABT:** m.p. 180 °C, yield 63%. The purity of the product ABT was checked by elemental analysis [Calcd.(Found)% for  $\text{C}_9\text{H}_{10}\text{N}_4\text{S}$  (ABT) M.Wt.=206.27; C 52.41(52.13); H 4.89(4.71); N 27.16(27.50); S 15.55(15.73)].

**BBT:** m.p. 182°C, yield 65%. The purity of BBT was checked by elemental analysis [Calcd.(Found)% for  $\text{C}_{16}\text{H}_{14}\text{N}_4\text{S}$ (BBT) M.Wt.=294.38; C 65.28 (64.98); H 4.79 (4.71); N 19.03 (18.93); S 10.89 (10.71)].

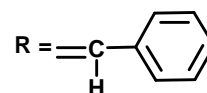
**HBHT:** m.p. 200°C, yield 61%. The purity of HBHT was checked by elemental analysis [Calcd.(Found)% for  $\text{C}_{16}\text{H}_{14}\text{N}_4\text{SO}$ (HBHT) M.Wt.=310.38; C 61.92(61.75); H 4.55(4.64); N 18.05(17.99); S 10.33 (9.88)].

**BMT:** m.p. 191-192°C, yield 59%. The purity of BMT was checked by elemental analysis [Calcd.(Found)% for  $\text{C}_{17}\text{H}_{16}\text{N}_4\text{SO}$ (BMT) M.Wt.=324.408; C 62.94(62.58); H 4.97(4.69); N 17.27(17.05); S 9.88(10.02)].

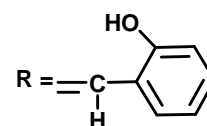
The structure of the ligands is given in Figure 1.



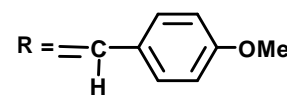
where: R =  $\text{H}_2$ ; 4-amino-5-benzyl-4H-1,2,4-triazole-3-thione (ABT),



5-benzyl-4-(benzylideneamino)-4H-1,2,4-triazole-3-thione (BBT)



5-benzyl-4-[(2-hydroxybenzylidene)amino]-4H-1,2,4-triazole-3-thione (HBHT)



5-benzyl-4-[(4-methoxybenzylidene)amino]-4H-1,2,4-triazole-3-thione (BMT)

Figure 1 : Structural representation of the ligands

### 2.2 Preparation and characterization of the Cu(II) complexes

*Cu(II) complexes* prepared according to the literature procedure<sup>[27]</sup>. Elemental analyses of the solid complexes were performed in an Elementar analyser system Gmbh Vario El. Electronic spectra were run on a Perkin Elmer UV/VIS spectrophotometer Lambda 40 using 1-cm matched silica cells. IR spectra were obtained in KBr discs using 470 Shimadzu infrared spectrophotometer ( $4000\text{-}400\text{ cm}^{-1}$ ). Conductivity measurements were carried out using CDM216 Meterlab conductivity meter in DMF solutions at  $10^{-3}$  M concentrations at room temperature ( $\sim 25^\circ\text{C}$ ). Magnetic susceptibility measurements were carried out at room temperature using a magnetic susceptibility balance of the type MSB-Auto. Molar susceptibilities were corrected for diamagnetism of the component atoms by the use of Pascal's constants. The calibrant used was  $\text{Hg}[\text{Co}(\text{SCN})_4]$ .

### 2.3. Thermal measurements

Thermogravimetric analyses of the various complexes was carried out using a Shimadzu DTG 60-H

thermal analyzer, at heating rate  $10\text{ }^{\circ}\text{C min}^{-1}$ , sample weight 5-6 mg and in a dynamic nitrogen atmosphere. The measured curves obtained during TGA scanning were analysed to give the percentage mass loss as a function of temperature. The different kinetic parameters were computed from thermal decomposition data using Coats-Redfern and Horowitz-Metzger methods<sup>[24,25]</sup>:

### Coats-Redfern equation

$$\ln\left[\frac{1-(1-\alpha)^{1-n}}{(1-n)T^2}\right] = \frac{M}{T} + B \quad \text{for } n \neq 1 \quad (1)$$

$$\ln\left[\frac{-\ln(1-\alpha)}{T^2}\right] = \frac{M}{T} + B \quad \text{for } n = 1 \quad (2)$$

where  $\alpha$  is the fraction of material decomposed,  $n$  is the order of the decomposition reaction and  $M = E^{\#}/R$  and  $B = ZR/\phi E^{\#}$ ;  $E^{\#}$ ,  $R$ ,  $Z$  and  $\phi$  are the activation energy, molar gas constant, pre-exponential factor (collision factor) and heating rate, respectively.

### Horowitz-Metzger equation

$$\ln\left[\frac{1-(1-\alpha)^{1-n}}{1-n}\right] = \ln\frac{ZRT_s^2}{\phi E^{\#}} - \frac{E^{\#}}{RT_s} + \frac{E^{\#}\theta}{RT_s^2} \quad \text{for } n \neq 1 \quad (3)$$

$$\ln[-\ln(1-\alpha)] = \frac{E^{\#}\theta}{RT_s^2} \quad \text{for } n = 1 \quad (4)$$

where  $\theta = T - T_s$ ,  $T_s$  is the temperature at the DTG peak.

The correlation coefficient  $r$ , was computed using the least squares method for different values of  $n$ , by plotting the left hand side of equation (1) and (2) against  $1/T$  and against  $\theta$  for equations (3) and (4). Linear relationships were obtained for different values of  $n$  ranging from 0 to 2. The value of  $n$ , which gave the best fit ( $r \sim 1$ ) was chosen as the order parameter for the decomposition stage of interest. From the intercept and linear slope of such stage, the kinetic parameters  $E^{\#}$  and  $Z$  were calculated.

Thermodynamic parameters: entropy ( $\Delta S^{\#}$ ), enthalpy ( $\Delta H^{\#}$ ) and free energy ( $\Delta G^{\#}$ ) of activation were calculated using the following standard relations<sup>[26]</sup>:

$$\Delta S^{\#} = R \left( \ln \frac{Zh}{kT_s} \right) \quad (5)$$

$$\Delta H^{\#} = \Delta E^{\#} + \Delta nRT_s \quad (6)$$

$$\Delta G^{\#} = \Delta H^{\#} - T_s \Delta S^{\#} \quad (7)$$

where:  $h$ , Planck's constant;  $k$ , Boltzmann constant;  $R$ , Molar gas constant;  $T_s$ , Temperature at the DTG peak.

## 3. RESULTS AND DISCUSSION

### 3.1. Thermal decomposition studies

The analytical and IR data for the complexes are resumed in TABLE 1 and 2 respectively. The spectral data with the magnetic moment values confirm the re-

TABLE 1 : Analytical and physical data for the complexes

No.	Complex Empirical Formula(F.Wt.)	Color	Yield (%)	Analysis Data, Found(Calcd.) %				$\Lambda_m^*$	$\mu_{eff}^{**}$
				C	H	N	S		
1	[Cu(ABT).2H <sub>2</sub> O]Cl <sub>2</sub>	Greenish	48	28.70	3.51	15.15	8.23	131.70	2.21
	C <sub>9</sub> H <sub>14</sub> Cl <sub>2</sub> CuN <sub>4</sub> SO <sub>2</sub> (376.75)	brown		(28.69)	(3.75)	(14.87)	(8.51)		
2	[Cu(ABT) <sub>2</sub> .2H <sub>2</sub> O]Cl <sub>2</sub>	Greenish	45	37.43	4.04	19.60	10.91	134.80	2.23
	C <sub>18</sub> H <sub>24</sub> Cl <sub>2</sub> CuN <sub>8</sub> S <sub>2</sub> O <sub>2</sub> (583.02)	brown		(37.08)	(4.15)	(19.22)	(10.99)		
3	[Cu(BBT) <sub>2</sub> Cl <sub>2</sub> ]	Green	47	52.80	3.83	15.60	8.74	36.70	-
	C <sub>32</sub> H <sub>28</sub> Cl <sub>2</sub> CuN <sub>8</sub> S <sub>2</sub> (723.20)			(53.14)	(3.90)	(15.49)	(8.87)		
4	[Cu(BHT)Cl.2H <sub>2</sub> O]	Green	49	43.36	4.07	12.80	7.43	25.50	-
	C <sub>16</sub> H <sub>17</sub> ClCuN <sub>4</sub> SO <sub>3</sub> (444.40)			(43.24)	(3.86)	(12.61)	(7.22)		
5	[Cu(BHT) <sub>2</sub> ]4H <sub>2</sub> O	Green	45	51.05	4.76	14.97	8.31	29.40	-
	C <sub>32</sub> H <sub>34</sub> CuN <sub>8</sub> S <sub>2</sub> O <sub>6</sub> (754.34)			(50.95)	(4.54)	(14.85)	(8.50)		
6	[Cu(BMT)Cl <sub>2</sub> ]0.5H <sub>2</sub> O	Green	47	43.63	3.94	12.14	6.98	37.20	1.86
	C <sub>17</sub> H <sub>17</sub> Cl <sub>2</sub> CuN <sub>4</sub> SO <sub>1.5</sub> (467.86)			(43.64)	(3.66)	(11.98)	(6.85)		
7	[Cu(BMT) <sub>2</sub> Cl <sub>2</sub> ]	White	45	52.05	3.84	14.09	7.96	27.20	-
	C <sub>34</sub> H <sub>32</sub> Cl <sub>2</sub> CuN <sub>8</sub> S <sub>2</sub> O <sub>2</sub> (783.25)			(52.14)	(4.12)	(14.31)	(8.19)		

\*Measured in DMF (Ohm<sup>-1</sup> cm<sup>2</sup> mol<sup>-1</sup>),

\*\* $\mu_{eff}$  in Bohr magneton, - : diamagnetic

## Full Paper

ported structure for these complexes<sup>[27]</sup>. The thermal analysis of the Cu(II) complexes in nitrogen atmosphere show 2-4 decomposition steps (Figure 2-16 and

TABLE 3), the kinetic and thermodynamic parameters are indicated in TABLE 4.

TABLE 2 : Relevant IR spectral data for ligands and their complexes (cm<sup>-1</sup>)

Compound	ν(O-H) (H <sub>2</sub> O)	ν(NH)	ν(C=N) Azo- methine	Thioamide bands			
				I δ(C-H)+ δ(N-H)	II ν(C=S)+ ν(C-N)+ δ(C-H)	III ν(C-N)+ ν(C-S)	IV ν(C=S)
Free ABT	-	3282	-	1565	1290	1040	793
[Cu(ABT).2H <sub>2</sub> O]Cl <sub>2</sub>	3427	3260	-	1545	1305	979	737
[Cu(ABT) <sub>2</sub> .2H <sub>2</sub> O]Cl <sub>2</sub>	3427	3260	-	1549	1300	1020	737
Free BBT	-	3100	1619	1588	1290	1008	794
[Cu(BBT) <sub>2</sub> Cl <sub>2</sub> ]	-	3040	1596	1578	1350	960	754
Free BHT	3400*	3102	1621	1582	1290	1008	814
[Cu(BHT)Cl.2H <sub>2</sub> O]	3408	3061	1600	1572	1343	968	745
[Cu(BHT) <sub>2</sub> ]4H <sub>2</sub> O	3408	3030	1600	1576	1355	980	758
Free BMT	-	3101	1623	1580	1282	1022	780
[Cu(BMT)Cl <sub>2</sub> ]0.5H <sub>2</sub> O	3450	3080	1592	1560	1304	976	726
[Cu(BMT) <sub>2</sub> Cl <sub>2</sub> ]	-	3080	1592	1564	1317	968	714

\*Phenolic ν(O-H) of the hydroxyl group

TABLE 3 : Thermal analytical data for the complexes

No.	Complex	Temp. range °C	Steps No.	Weight loss %		Loss of moiety	Process	Residue	
				Calcd.	Found			Calcd. (Found) %	Nature
1	[Cu(ABT).2H <sub>2</sub> O]Cl <sub>2</sub>	100-220 223-629 630-750	I	9.56	9.72	2H <sub>2</sub> O	Dehydration	29.61(29.73)	CuS—NH <sub>2</sub>
			II + III	42.99	42.99	C <sub>7</sub> H <sub>7</sub> + 2Cl	Decomposition		
			IV	17.78	17.56	C <sub>2</sub> HN <sub>3</sub>	Decomposition		
2	[Cu(ABT) <sub>2</sub> .2H <sub>2</sub> O]Cl <sub>2</sub>	83-213 221-425 426-750	I	6.17	6.01	2H <sub>2</sub> O	Dehydration	38.86(38.78)	CuS—C <sub>2</sub> H <sub>5</sub> N <sub>5</sub> S
			II	27.79	28.93	C <sub>7</sub> H <sub>7</sub> + 2Cl	Decomposition		
			III	27.1	27.28	C <sub>7</sub> H <sub>7</sub> + C <sub>2</sub> HN <sub>3</sub>	Decomposition		
3	[Cu(BBT) <sub>2</sub> Cl <sub>2</sub> ]	114-495 496-701	I	59.9	59.75	2C <sub>7</sub> H <sub>6</sub> + 2C <sub>7</sub> H <sub>7</sub> + 2Cl	Decomposition	17.64 (17.69)	CuS—S
			II	22.4	22.56	C <sub>4</sub> H <sub>2</sub> N <sub>8</sub>	Decomposition		
4	[Cu(BHT)Cl.2H <sub>2</sub> O]	140-235 255-750	I	8.1	7.92	2H <sub>2</sub> O	Dehydration	30.72(30.83)	CuS—CHN <sub>2</sub>
			II + III	61.09	61.25	C <sub>7</sub> H <sub>7</sub> + C <sub>7</sub> H <sub>5</sub> O + CN <sub>2</sub> + Cl	Decomposition		
			II	51.97	52.13	2C <sub>7</sub> H <sub>6</sub> O + 2C <sub>7</sub> H <sub>7</sub>	Decomposition		
5	[Cu(BHT) <sub>2</sub> ]4H <sub>2</sub> O	57-171 205-483 487-750	I	9.54	9.69	4H <sub>2</sub> O	Dehydration	16.91(16.86)	CuS—S
			II	51.97	52.13	2C <sub>7</sub> H <sub>6</sub> O + 2C <sub>7</sub> H <sub>7</sub>	Decomposition		
			III	21.48	21.32	C <sub>4</sub> H <sub>2</sub> N <sub>8</sub>	Decomposition		
6	[Cu(BMT)Cl <sub>2</sub> ]0.5H <sub>2</sub> O	49-148 183-436 437-750	I	1.93	2.2	0.5H <sub>2</sub> O	Dehydration	23.42 (23.38)	CuS—N
			II	38.05	37.87	C <sub>7</sub> H <sub>7</sub> O + 2Cl	Decomposition		
			III	36.55	36.55	C <sub>10</sub> H <sub>9</sub> N <sub>3</sub>	Decomposition		
7	[Cu(BMT) <sub>2</sub> Cl <sub>2</sub> ]	216-348 349-623	I	62.98	63.12	2C <sub>8</sub> H <sub>8</sub> O + 2C <sub>7</sub> H <sub>7</sub> + 2Cl	Decomposition	10.16 (10.12)	CuO
			II	27.32	27.2	C <sub>3</sub> H <sub>2</sub> N <sub>8</sub> S <sub>2</sub>	Decomposition		

### 3.1.1. Thermal analysis of [Cu(ABT).2H<sub>2</sub>O]Cl<sub>2</sub>

The TGA of the square planar complex [Cu(ABT).2H<sub>2</sub>O]Cl<sub>2</sub> gave four steps (Figure 2). Coats-Redfern plots for the four decomposition steps of the complex are displayed in Figure 3. The first step (T =

100-220 °C, E<sup>#</sup> = 28.46 kJ/mol) is assignable to the removal of the two water molecules existing in the inner coordination sphere (Calcd. 9.56%, Found 9.72%). The second (T = 223-273 °C, E<sup>#</sup> = 62.91 kJ/mol) and third (T = 274-629 °C, E<sup>#</sup> = 35.61 kJ/mol) steps are assignable to the dissociation of the ABT ligand with

the removal of C<sub>7</sub>H<sub>7</sub> moiety and two chlorine atoms (Calcd. 42.99%, Found 42.99%). The fourth step (T = 630-750°C, E<sup>#</sup> = 25.58 kJ/mol) corresponds to the progress of the dissociation of the ABT ligand, with the removal of C<sub>2</sub>HN<sub>3</sub> moiety (Calcd. 17.78%, Found

17.56%), leading to the final residue CuS—NH<sub>2</sub> (Calcd. 29.61%, Found 29.73%).

The suggested mechanism for the thermal pyrolysis of this complex can therefore be represented as follows:

TABLE 4 : Kinetic and thermodynamic parameters for the thermal decomposition of copper(II) complexes using non-mechanistic equation in nitrogen flow

Complex (No.)	Step	n	Coats-Redfern equation Thermodynamic (Kinetic parameters) parameters						Horowitz-Metzger equation Thermodynamic (Kinetic parameters) parameters					
			r	E <sup>#</sup>	Z	ΔS <sup>#</sup> x 10 <sup>-2</sup>	ΔH <sup>#</sup> x 10 <sup>-3</sup>	ΔG <sup>#</sup> x 10 <sup>-5</sup>	r	E <sup>#</sup>	Z	ΔS <sup>#</sup> x 10 <sup>-2</sup>	ΔH <sup>#</sup> x 10 <sup>-3</sup>	ΔG <sup>#</sup> x 10 <sup>-5</sup>
[Cu(ABT).2H <sub>2</sub> O]Cl <sub>2</sub> (1)	1 <sup>st</sup>	1.00	0.9984	28.46	9.15 x 10 <sup>4</sup>	-1.54	3.90	0.75	0.9992	32.05	2.30 x 10 <sup>5</sup>	-1.27	3.90	0.63
	2 <sup>nd</sup>	2.00	0.9907	62.91	8.05 x 10 <sup>11</sup>	-0.22	4.30	0.15	0.9920	67.61	7.88 x 10 <sup>12</sup>	-0.02	4.31	0.06
	3 <sup>rd</sup>	2.00	0.9995	35.61	3.62 x 10 <sup>3</sup>	-1.83	5.07	1.16	0.9980	41.34	3.01 x 10 <sup>4</sup>	-1.65	5.08	1.05
	4 <sup>th</sup>	0.33	0.9997	25.58	2.60 x 10 <sup>6</sup>	-1.32	7.87	1.32	1.0000	37.61	7.99 x 10 <sup>5</sup>	-2.56	7.88	2.50
[Cu(ABT) <sub>2</sub> .2H <sub>2</sub> O]Cl <sub>2</sub> (2)	1 <sup>st</sup>	0.66	0.9920	9.83	1.16 x 10 <sup>4</sup>	-1.70	3.73	0.80	0.9961	12.92	2.26 x 10 <sup>4</sup>	-2.22	3.73	1.03
	2 <sup>nd</sup>	2.00	0.9992	60.41	6.14 x 10 <sup>10</sup>	-0.43	4.42	0.27	0.9995	64.03	3.78 x 10 <sup>11</sup>	-0.28	4.42	0.19
	3 <sup>rd</sup>	2.00	0.9990	25.11	1.28 x 10 <sup>6</sup>	-1.37	7.19	1.25	0.9997	34.67	1.22 x 10 <sup>5</sup>	-2.52	7.20	2.24
[Cu(BBT) <sub>2</sub> Cl <sub>2</sub> ] (3)	1 <sup>st</sup>	0.33	0.9997	21.72	1.11 x 10 <sup>3</sup>	-1.91	4.42	1.06	1.0000	26.63	1.33 x 10 <sup>3</sup>	-1.90	4.43	0.04
	2 <sup>nd</sup>	0.33	0.9553	47.07	1.51 x 10 <sup>4</sup>	-1.73	6.86	1.49	0.9969	53.83	2.11 x 10 <sup>2</sup>	-2.09	6.86	1.78
[Cu(BHT)Cl.2H <sub>2</sub> O] (4)	1 <sup>st</sup>	1.00	0.9989	15.05	3.78 x 10 <sup>3</sup>	-1.80	3.91	0.88	0.9998	18.30	3.12 x 10 <sup>2</sup>	-2.01	3.91	0.98
	2 <sup>nd</sup>	2.00	0.9963	50.75	3.25 x 10 <sup>6</sup>	-1.26	4.82	0.77	0.9937	56.61	3.74 x 10 <sup>7</sup>	-1.05	4.82	0.65
	3 <sup>rd</sup>	2.00	0.9979	38.61	7.83 x 10 <sup>4</sup>	-1.59	6.51	1.30	0.9988	47.91	5.63 x 10 <sup>5</sup>	-2.19	6.52	1.77
[Cu(BHT) <sub>2</sub> ]4H <sub>2</sub> O (5)	1 <sup>st</sup>	2.00	0.9983	32.12	6.51 x 10 <sup>9</sup>	-0.60	3.54	0.29	0.9998	35.06	7.54 x 10 <sup>10</sup>	-0.40	3.54	0.20
	2 <sup>nd</sup>	2.00	0.9951	29.55	1.51 x 10 <sup>4</sup>	-1.69	4.26	0.91	0.9921	33.47	1.10 x 10 <sup>5</sup>	-1.53	4.27	0.82
	3 <sup>rd</sup>	2.00	0.9977	60.41	4.88 x 10 <sup>3</sup>	-1.84	7.80	1.79	0.9997	68.88	1.03 x 10 <sup>3</sup>	-1.97	7.81	1.91
[Cu(BMT)Cl <sub>2</sub> ]0.5H <sub>2</sub> O (6)	1 <sup>st</sup>	1.00	0.9990	12.59	1.12 x 10 <sup>3</sup>	-1.90	3.61	0.86	0.9979	15.22	7.21 x 10 <sup>2</sup>	-1.93	3.61	0.87
	2 <sup>nd</sup>	0.33	0.9993	15.25	1.28 x 10 <sup>4</sup>	-1.71	4.23	0.91	0.9999	19.10	4.16 x 10 <sup>1</sup>	-2.18	4.24	1.15
	3 <sup>rd</sup>	1.00	0.9996	70.86	5.72 x 10 <sup>3</sup>	-1.82	7.01	1.59	0.9999	81.15	1.27 x 10 <sup>5</sup>	-1.56	7.02	1.37
[Cu(BMT) <sub>2</sub> Cl <sub>2</sub> ] (7)	1 <sup>st</sup>	1.00	0.9999	34.67	3.52 x 10 <sup>4</sup>	-1.63	4.44	0.91	0.9997	39.12	7.87 x 10 <sup>5</sup>	-1.37	4.45	0.77
	2 <sup>nd</sup>	0.50	0.9892	36.69	7.44 x 10 <sup>4</sup>	-1.60	6.74	1.36	0.9999	46.93	6.26 x 10 <sup>5</sup>	-2.19	6.75	1.83

E<sup>#</sup> in kJmol<sup>-1</sup>, Z in s<sup>-1</sup>, ΔH<sup>#</sup> and ΔG<sup>#</sup> in kJmol<sup>-1</sup> & ΔS<sup>#</sup> in kJmol<sup>-1</sup>K<sup>-1</sup>

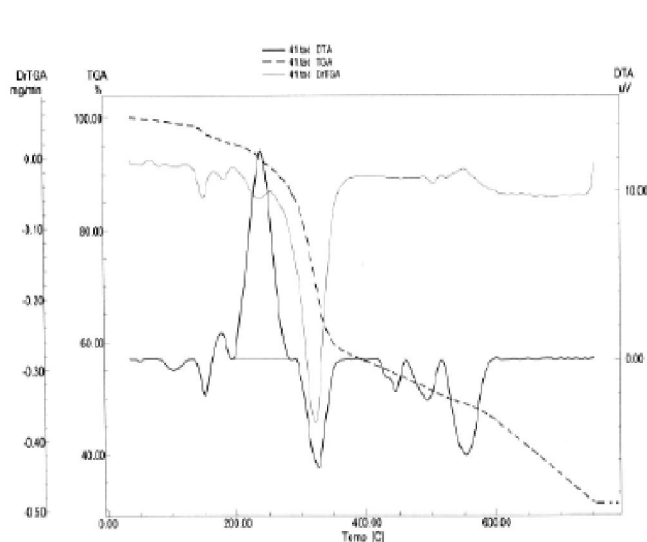
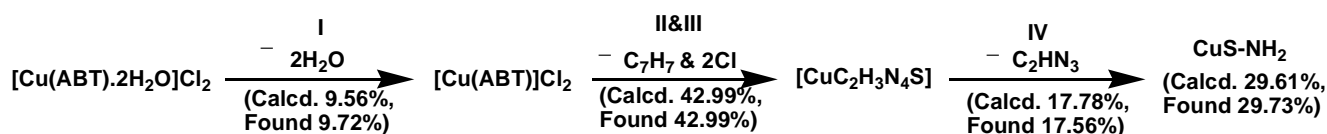


Figure 2 : TG-DTG curves of [Cu(ABT).2H<sub>2</sub>O]Cl<sub>2</sub>

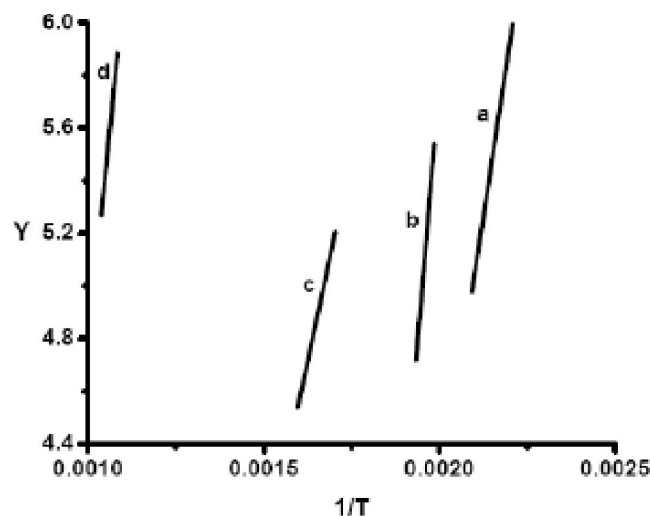


Figure 3 : Coats-Redfern plots for the four decomposition steps: a) first step b) second step c) third step d) fourth step

## Full Paper

### 3.1.2. Thermal analysis of $[\text{Cu}(\text{ABT})_2 \cdot 2\text{H}_2\text{O}]\text{Cl}_2$

The octahedral complex  $[\text{Cu}(\text{ABT})_2 \cdot 2\text{H}_2\text{O}]\text{Cl}_2$  has a TGA displays three decomposition steps (Figure 4). Coats-Redfern and Horowitz-Metzger plots for the three decomposition are represented in Figure 5 and 6 respectively. The first step ( $T = 83\text{-}213^\circ\text{C}$ ,  $E^\# = 9.83$  kJ/mol) is assignable to the removal of two water molecules, existing in the inner coordination sphere (Calcd. 6.17%, Found 6.01%). The second step ( $T = 221\text{-}$

$425^\circ\text{C}$ ,  $E^\# = 60.41$  kJ/mol) is assignable to the dissociation of the ABT ligand with the removal of one  $\text{C}_7\text{H}_7$  moiety and two chlorine atoms (Calcd. 27.79%, Found 27.93%). The third step ( $T = 426\text{-}750^\circ\text{C}$ ,  $E^\# = 25.11$  kJ/mol) corresponds to further dissociation of the ABT ligands through the loss of  $\text{C}_7\text{H}_7$  and  $\text{C}_2\text{HN}_3$  moieties (Calcd. 27.10%, Found 27.28%), leading to the final residue  $\text{CuS}-\text{C}_2\text{H}_5\text{N}_5\text{S}$  (Calcd. 38.86%, Found 38.78%). The thermal decomposition chemistry of this complex may be expressed as follows:

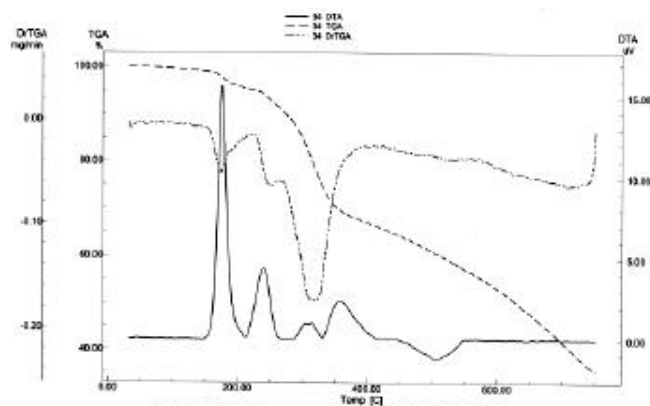
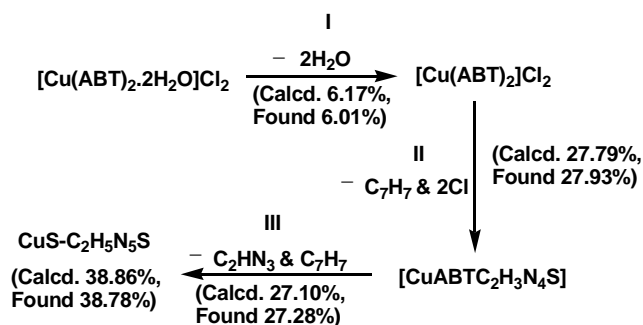


Figure 4 : TG-DTG curves of  $[\text{Cu}(\text{ABT})_2 \cdot 2\text{H}_2\text{O}]\text{Cl}_2$

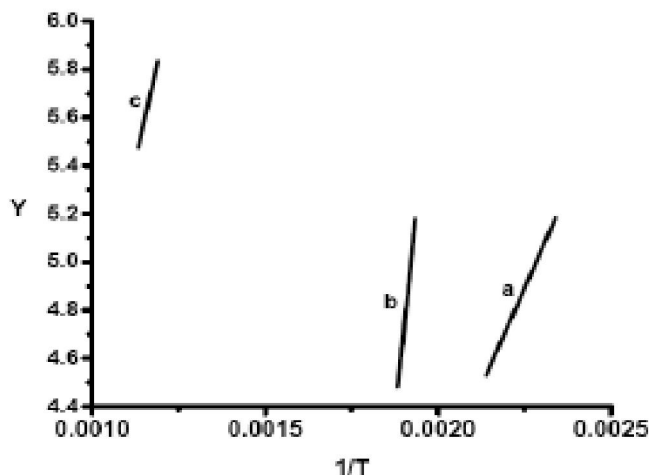


Figure 5 : Coats-Redfern plots for the three decomposition steps: a) first step b) second step c) third step

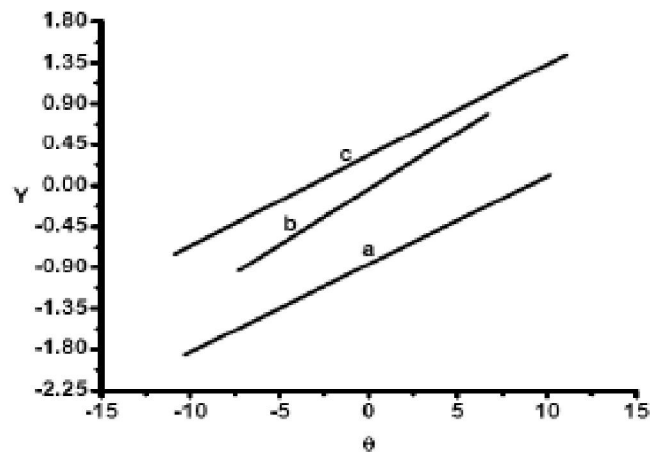


Figure 6 : Horowitz-Metzger plots for the three decomposition steps: a) first step b) second step c) third step

### 3.1.3. Thermal analysis of $[\text{Cu}(\text{BBT})_2]\text{Cl}_2$

The thermogram of the octahedral complex  $[\text{Cu}(\text{BBT})_2]\text{Cl}_2$  exhibited two decomposition steps (Figure 7). Horowitz-Metzger plots for the two decomposition steps are shown in Figure 8. The first step ( $T = 114\text{-}495^\circ\text{C}$ ,  $E^\# = 21.72$  kJ/mol) is assignable to the dissociation of the BBT ligands with the

removal of two  $\text{C}_7\text{H}_6$  and two  $\text{C}_7\text{H}_7$  moieties, one from each BBT molecule and two chlorine atoms (Calcd. 59.90%, Found 59.75%). The second step ( $T = 496\text{-}701^\circ\text{C}$ ,  $E^\# = 47.07$  kJ/mol) is assignable to the progress of the dissociation of the BBT ligands, with the removal of  $\text{C}_4\text{H}_2\text{N}_8$  (Calcd. 22.40%, Found 22.56%), leading to the final residue  $\text{CuS}-\text{S}$  (Calcd.

17.64%, Found 17.69%). The following diagram represents a detailed description of the mechanism and

the species resulted in the thermal decomposition of this complex:

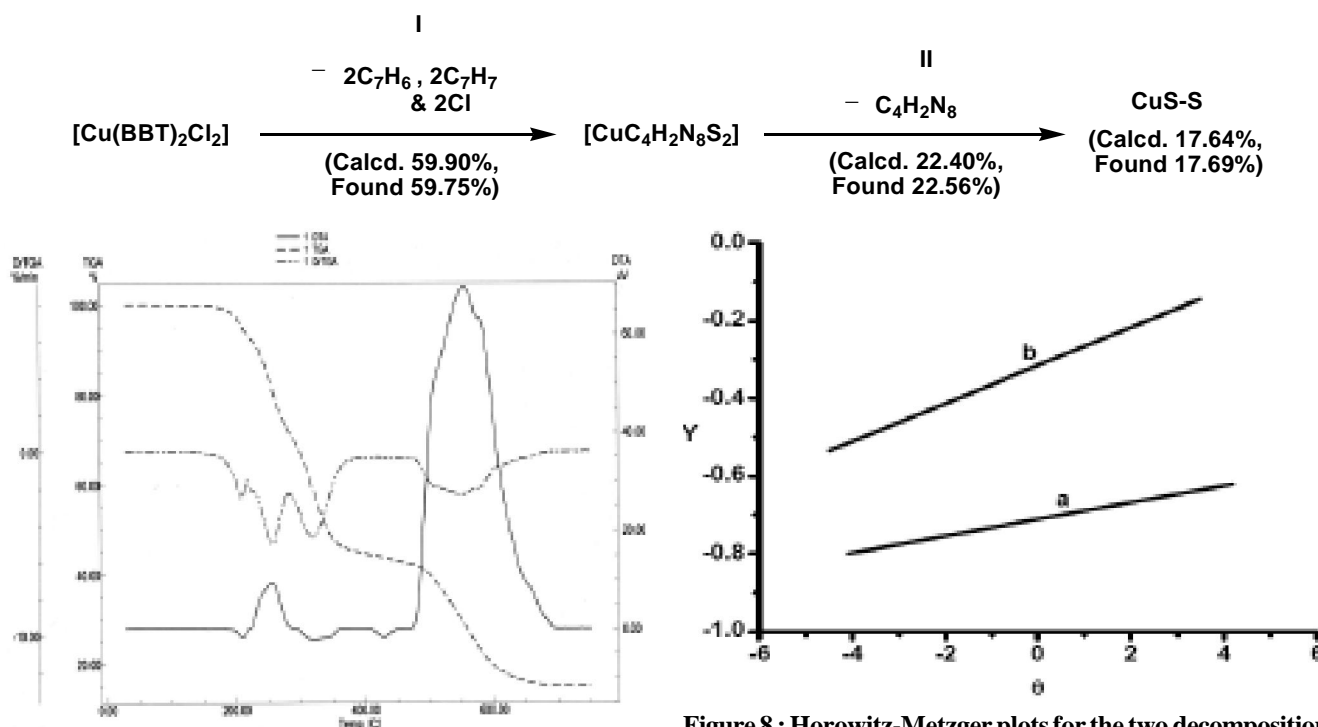
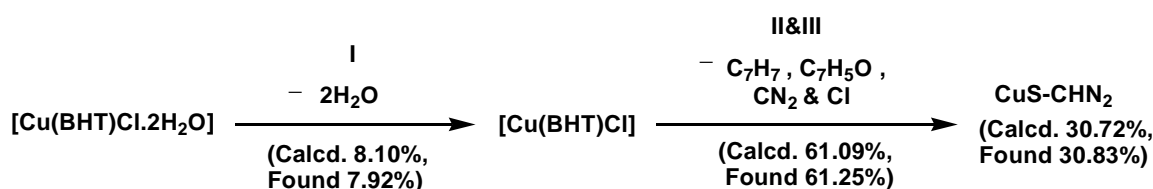


Figure 7 : TG-DTG curves of  $[\text{Cu}(\text{BBT})_2\text{Cl}_2]$

### 3.1.4. Thermal analysis of $[\text{Cu}(\text{BHT})\text{Cl}\cdot 2\text{H}_2\text{O}]$

TGA of the complex  $[\text{Cu}(\text{BHT})\text{Cl}\cdot 2\text{H}_2\text{O}]$  displays three decomposition steps. The first step ( $T = 140\text{--}235^\circ\text{C}$ ,  $E^\ddagger = 15.05\text{ kJ/mol}$ ) is assignable to the removal of two water molecules, existing in the inner coordination sphere (Calcd. 8.10%, Found 7.92%). The second ( $T = 255\text{--}431^\circ\text{C}$ ,  $E^\ddagger = 50.75\text{ kJ/mol}$ ) and third steps ( $T =$

$433\text{--}750^\circ\text{C}$ ,  $E^\ddagger = 38.61\text{ kJ/mol}$ ) are assignable to the dissociation of BHT ligand through the removal of  $\text{C}_7\text{H}_7$ ,  $\text{C}_7\text{H}_5\text{O}$  and  $\text{CN}_2$  moieties and one chlorine atom (Calcd. 61.09%, Found 61.25%), leading to the final residue  $\text{CuS}\text{—CHN}_2$  (Calcd. 30.72%, Found 30.83%). The different decomposition steps for this complex could be given according to the following proposed mechanism:



### 3.1.5. Thermal analysis of $[\text{Cu}(\text{BHT})_2]\cdot 4\text{H}_2\text{O}$

Thermogravimetric analysis of the octahedral complex  $[\text{Cu}(\text{BHT})_2]\cdot 4\text{H}_2\text{O}$  shows three decomposition steps (Figure 9). Horowitz-Metzger plots for the three decomposition steps are displayed in Figure 10. The first step ( $T = 57\text{--}171^\circ\text{C}$ ,  $E^\ddagger = 32.12\text{ kJ/mol}$ ) is assignable to the removal of four lattice water molecules (Calcd. 9.54%, Found 9.69%).

The second step ( $T = 205\text{--}483^\circ\text{C}$ ,  $E^\ddagger = 29.55\text{ kJ/mol}$ ) is assignable to the dissociation of the two BHT molecules through the removal of two  $\text{C}_7\text{H}_5\text{O}$  and two  $\text{C}_7\text{H}_7$  moieties (Calcd. 51.97%, Found 52.13%). The third step ( $T = 487\text{--}750^\circ\text{C}$ ,  $E^\ddagger = 60.41\text{ kJ/mol}$ ) is corresponding to further decomposition of the BHT ligand with the removal of  $\text{C}_4\text{H}_2\text{N}_8$  moiety (Calcd. 21.48%, Found 21.32%),

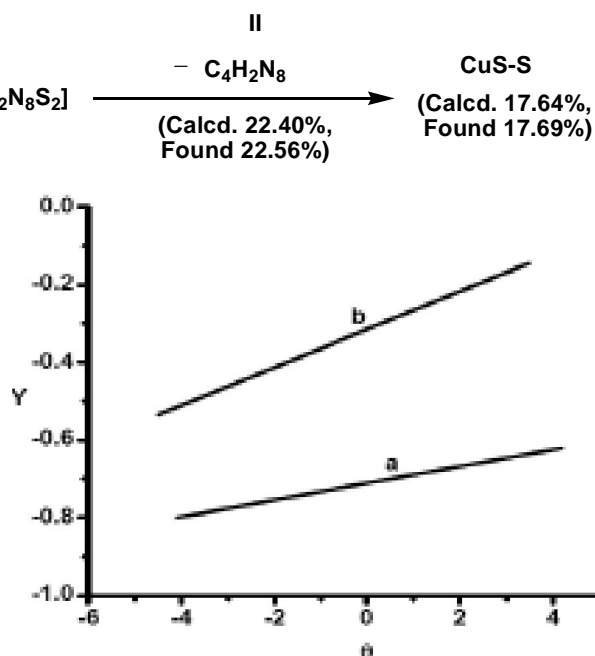


Figure 8 : Horowitz-Metzger plots for the two decomposition steps: a) first step b) second step

## Full Paper

leading to the final residue CuS—S (Calcd. 16.91%, Found 16.86%).

The mechanism of the effect of temperature on this complex is represented in the following scheme:

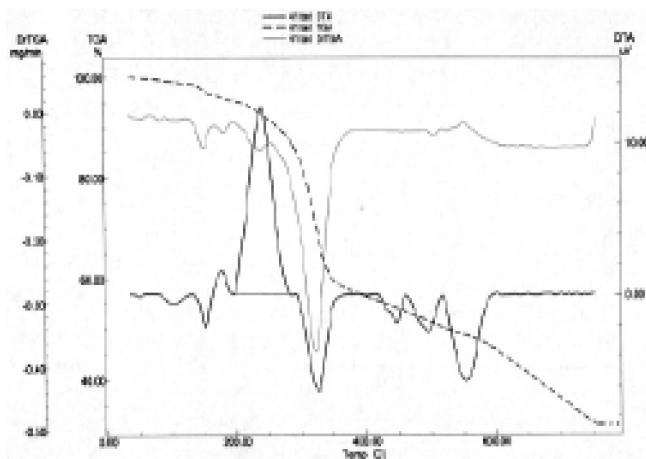
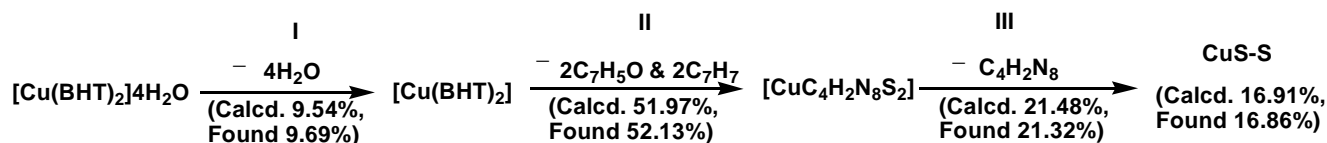


Figure 9 : TG-DTG curves of [Cu(BHT)<sub>2</sub>]4H<sub>2</sub>O

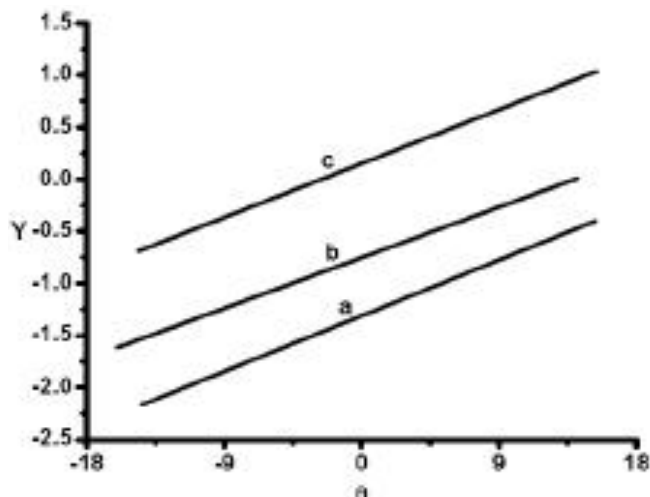


Figure 10 : Horowitz-Metzger plots for the three decomposition steps: a) first step b) second step c) third step

### 3.1.6. Thermal analysis of [Cu(BMT)Cl<sub>2</sub>]0.5H<sub>2</sub>O

The square planar [Cu(BMT)Cl<sub>2</sub>]0.5H<sub>2</sub>O complex display three decomposition steps (Figure 11). Coats-Redfern and Horowitz-Metzger plots for the three decomposition are represented in Figure 12 and 13 respectively. The first step (T = 49-148 °C, E<sup>#</sup> = 12.59 kJ/mol) is assignable to the removal of half water molecule, existing outer the coordination sphere (Calcd. 1.93%, Found 2.20%). The second step (T = 183-436 °C, E<sup>#</sup> =

15.25 kJ/mol) is assignable to the dissociation of BMT ligand with the removal of C<sub>7</sub>H<sub>7</sub>O moiety and two chlorine atoms (Calcd. 38.05%, Found 37.87%). The third step (T = 437-750 °C, E<sup>#</sup> = 70.86 kJ/mol) corresponds to the loss of C<sub>10</sub>H<sub>9</sub>N<sub>3</sub> moiety (Calcd. 36.55%, Found 36.55%), leading to the final residue CuS—N (Calcd. 23.42%, Found 23.38%). The different decomposition steps for this complex could be given according to the following proposed mechanism:

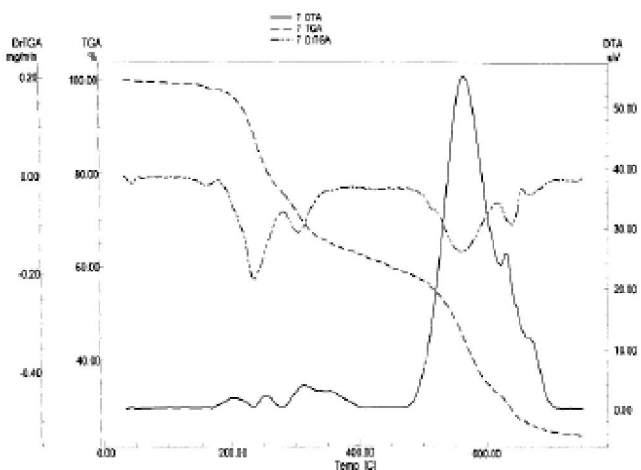
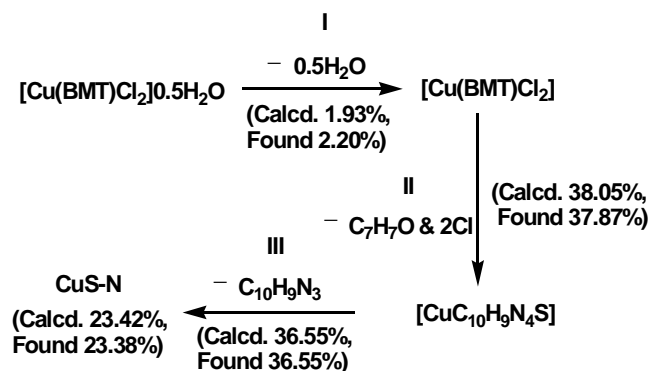


Figure 11 : TG-DTG curves of [Cu(BMT)Cl<sub>2</sub>]0.5H<sub>2</sub>O

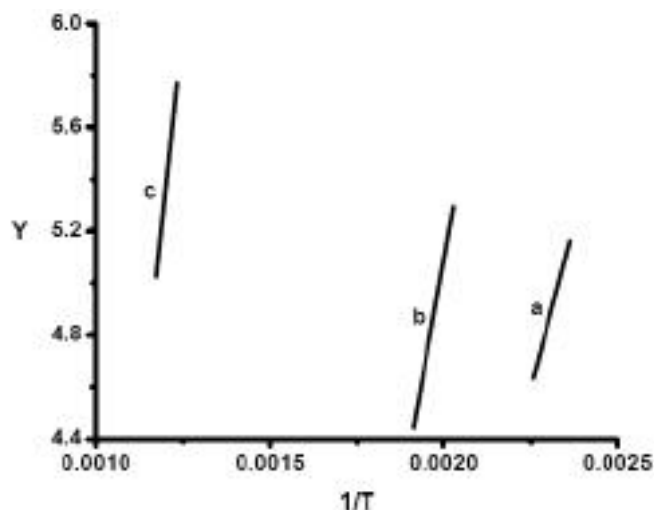


Figure 12 : Coats-Redfern plots for the three decomposition steps: a) first step b) second step c) third step

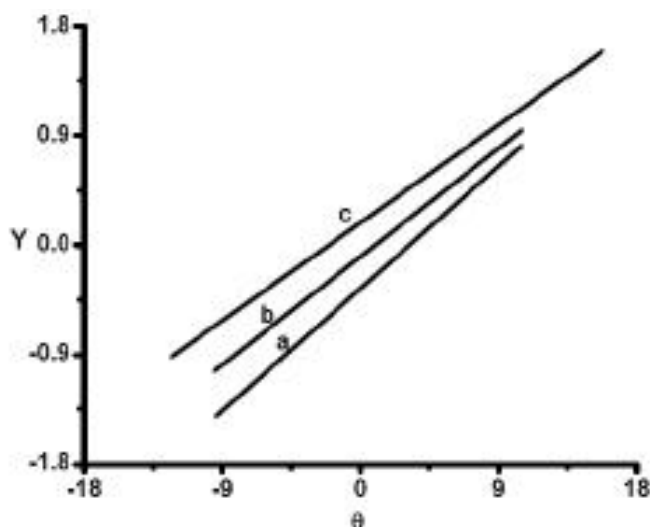


Figure 13 : Horowitz-Metzger plots for the three decomposition steps: a) first step b) second step c) third step

### 3.1.7. Thermal analysis of [Cu(BMT)<sub>2</sub>Cl<sub>2</sub>]

On the other hand the thermogram of the octahedral complex [Cu(BMT)<sub>2</sub>Cl<sub>2</sub>] exhibited two decomposition steps (Figure 14). Coats-Redfern and Horowitz-Metzger plots for the two decomposition are appeared in Figure 15 and 16 respectively. The first step (T = 216-348 °C, E<sup>#</sup> = 34.67 kJ/mol) is assignable to the dissociation of the BMT ligands with the removal of two C<sub>8</sub>H<sub>8</sub>O and

two C<sub>7</sub>H<sub>7</sub> moieties as well as two chlorine atoms (Calcd. 62.98%, Found 63.12%). The second step (T = 349-623 °C, E<sup>#</sup> = 36.69 kJ/mol) is assignable to the progress of the dissociation of BMT ligands with the removal of C<sub>3</sub>H<sub>2</sub>N<sub>8</sub>S<sub>2</sub> moiety (Calcd. 27.32%, Found 27.20%), leading to the final residue CuO (Calcd. 10.16%, Found 10.12%). The thermal decomposition chemistry of this complex may be expressed as follows:

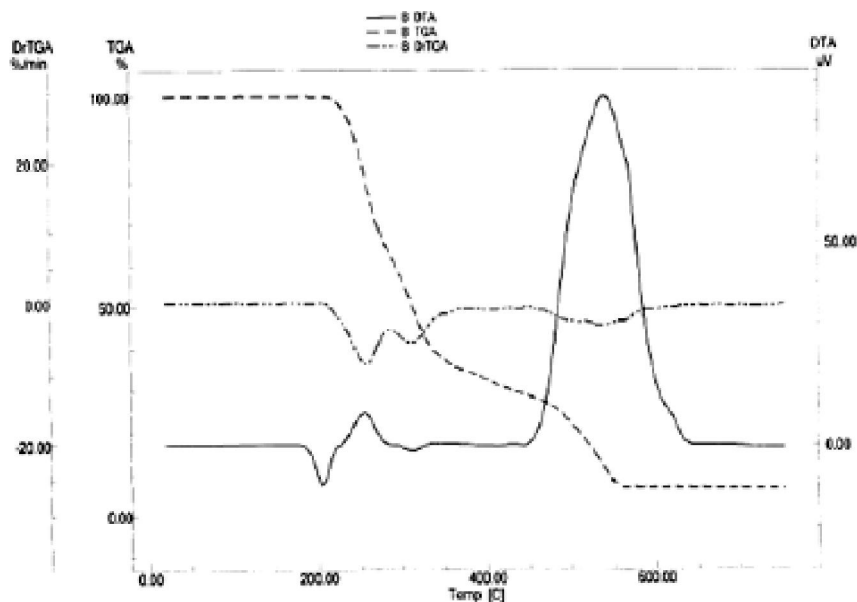
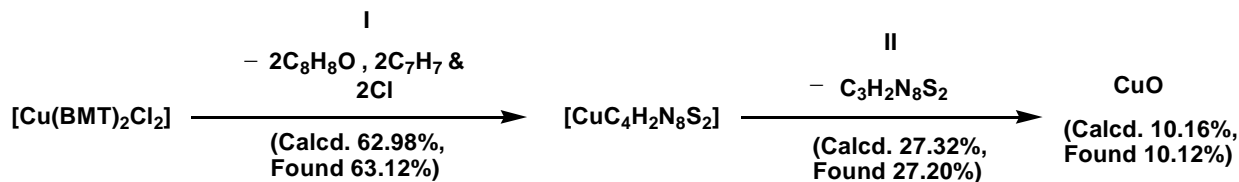


Figure 14 : TG-DTG curves of [Cu(BMT)<sub>2</sub>Cl<sub>2</sub>]

27.32%,  
27.20%)

## Full Paper

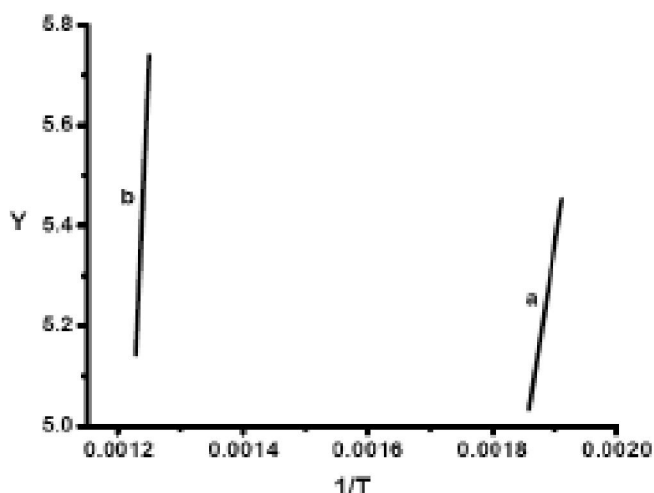


Figure 15 : Coats-Redfern plots for the two decomposition steps: a) first step b) second step

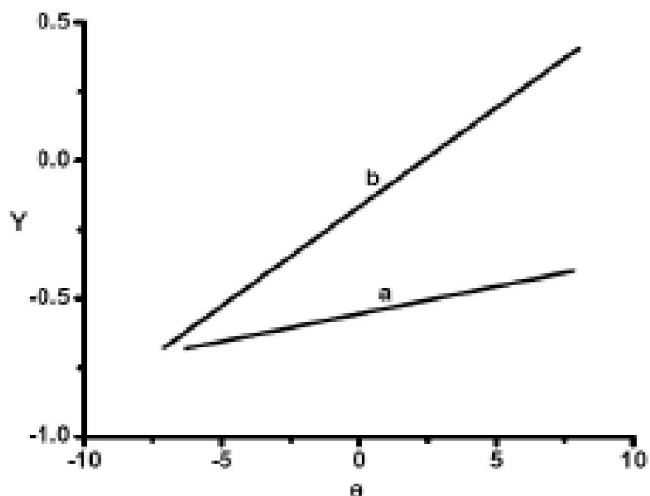


Figure 16 : Horowitz-Metzger plots for the two decomposition steps: a) first step b) second step

### 3.3. Thermal stability

Comparing the values of the initial decomposition temperatures ( $T_{i,dec.}$ ) of the organic part or the activation energy data for the isostructural copper(II) complexes  $[Cu(ABT)_2 \cdot 2H_2O]Cl_2$  (2),  $[Cu(BBT)_2Cl_2]$  (3),  $[Cu(BHT)_2]4H_2O$  (5) and  $[Cu(BMT)_2Cl_2]$  (7) indicates

that the complex (2) is the most thermally stable one while the complex (3) is the least stable one as appear in Figure 17 and TABLE 3. The initial decomposition temperatures and the activation energies for the beginning of the dissociation of the organic moiety indicate that the obtained complexes could be arranged in the following stability order:

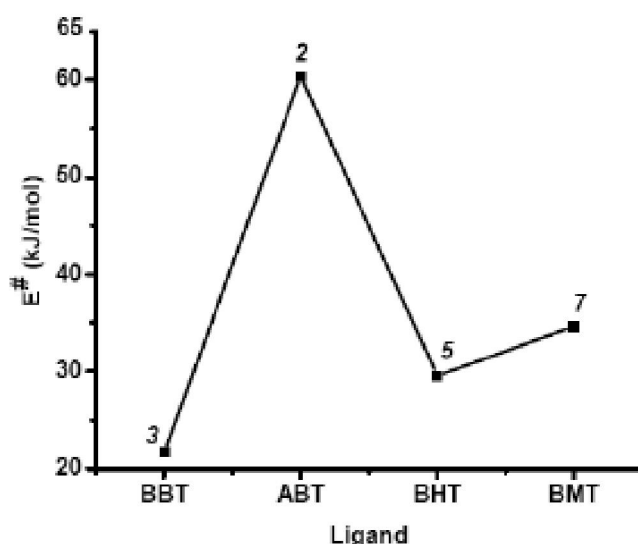
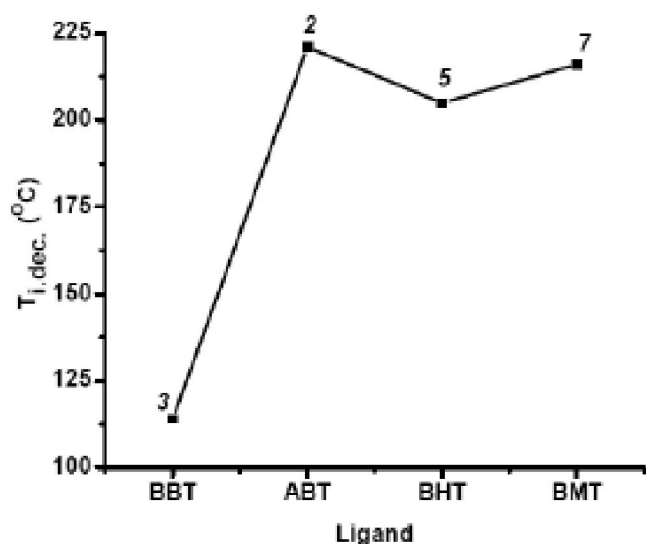
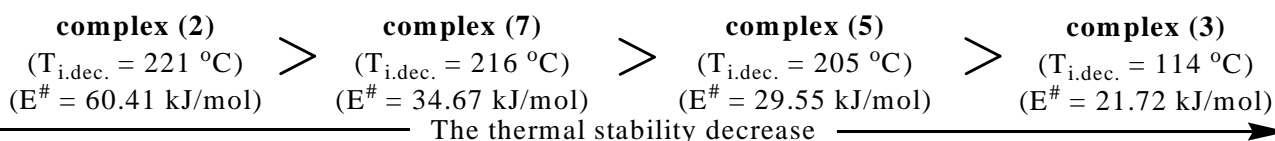


Figure 17 : Relationships between the initial decomposition temperature or activation energy and ligand type of copper(II) complexes

The thermal stability order of copper(II) complexes could be displayed by the following graph (Figure 17).

In view of these results, ABT complexes are the most stable ones, this may attributed to the structural

features of the ABT ligand. While the weakest coordination bonds are formed between the copper(II) ion and BBT ligand.

### 3.4. Conclusion remarks on the thermoanalytical data

The studied complexes have some common features in their thermal decomposition. These can be summarized as follows:

#### 3.4.1 TGA and DTA curves

Studying the TGA and DTA curves for the complexes indicates that there is a series of thermal changes on the DTA curves associate the weight loss in the TGA curves. This study leads to the following conclusions:

- (i) The presence of more than one exothermic peak in the DTA curves of all complexes reveals that the pyrolysis occurs in several steps<sup>[31]</sup>.
- (ii) The difference in the shape of the DTA curves of the binary complexes with respect to each other may attributed to the structural features of the ligand or the strength of the chelation between the metal ion and the ligand, this also led to the variety in the thermal behaviour of the complexes<sup>[32]</sup>.
- (iii) On heating the complexes containing water molecules from room temperature, the loss in weight indicated by the TGA curves is accompanied in some cases by endothermic peaks in the DTA curves. This weight loss may correspond to the evolution of water molecules<sup>[32]</sup>.
- (iv) The thermal behaviour of the complexes displays an observable difference with respect to each other. This difference indicates that the thermal behaviour of these complexes depends mainly on the type of the ligands rather than the type of the metal ion.
- (v) Some DTA curves of the anhydrous binary complexes start with an endothermic peaks. These endothermic DTA peaks are accompanied by a weight loss in the TGA curves which may attributed to phase change or structural rearrangement.
- (vi) Most complexes having DTA curves characterized by the presence of main sharp and strong exothermic peaks in their ends. These peaks are associated with a weight loss on the TGA curves corresponding to the decomposition of the stable

intermediate compounds into the corresponding final residue (metal oxide or metal sulfide depending on the type of ligand used)<sup>[32]</sup>.

#### 3.4.2. Thermodynamic parameters

The entropy ( $\Delta S^\ddagger$ ), enthalpy ( $\Delta H^\ddagger$ ) and free energy ( $\Delta G^\ddagger$ ) of activation were calculated for the complexes using standard equations<sup>[26]</sup> and the values are given in TABLE 4. The obtained data could be discussed as follow:

- (i) The entropy values for all degradation steps of all complexes were found to be negative, which indicates a more ordered activated state that may be possible through the chemisorption of oxygen and other decomposition products<sup>[14,17,33]</sup>.
- (ii) The relatively low values of  $\Delta H^\ddagger$  for copper(II) complexes confirm the M—S or M—N bond rupture<sup>[34,35]</sup>.
- (iii) The high values of the free energy of activation ( $\Delta G^\ddagger$ ) for most of the steps in the decomposition reactions of the complexes mean that the decomposition reactions are slower than that of the normal ones<sup>[26]</sup>.
- (iv) In general there are no obvious trends in the values of  $\Delta H^\ddagger$  and  $\Delta S^\ddagger$  for the studied complexes. This may attributed to the fact that the thermal decomposition of the complexes is controlled not only by the structure of the ligands but also by the configuration of the coordination sphere. The studied complexes comprise different types of ligands with bidentate or tridentate character; different structures around the metal ions were assumed (square planer or octahedral environments)<sup>[36,37]</sup>.
- (v) The values of the free energy of activation ( $\Delta G^\ddagger$ ) of a given complex, generally increase significantly for the subsequent decomposition stages. This is due to increasing the values of  $T\Delta S^\ddagger$  significantly from one step to another which overrides the values of  $\Delta H^\ddagger$ <sup>[26]</sup>.
- (vi) Increasing the values of  $\Delta G^\ddagger$  for the subsequent steps of a given complex reflects that the rate of removal of a given species will be lower than that of the precedent one<sup>[26]</sup>. This may attributed to the structure rigidity of the remaining complex.
- (vii) The similar values of  $\Delta G^\ddagger$  for the decomposition steps involving the same decomposition species

## Full Paper

and to some extent in structurally similar complexes reveal that the effect of the ligands is more pronounced than that of the divalent metal ions<sup>[26]</sup>.

- (viii) There is much closeness in the enthalpy ( $\Delta H^\ddagger$ ) values obtained by Coats-Redfern equation and Horowitz-Metzger equation, indicating that the thermal degradation of these complexes follow the standard methods.

### 3.4.3. Kinetic parameters and thermal behaviour

- (i) The thermal decomposition of the complexes is not simple and the processes generally involve overlapping steps which together with the great diversity of possible intermediate products precludes exhaustive interpretations. Although we successful in predicting and interpretation the thermal decomposition patterns for many complexes.
- (ii) The procedure for the thermal decomposition of the complexes resembles the thermal decomposition:  $A_{(s)} \rightarrow B_{(s)} + C_{(g)}$  which can be studied kinetically.
- (iii) All the complexes having a uniform decomposition pattern.
- (iv) In all complexes dehydration being the first step, whenever they containing water molecules, loss of the side chain of the ligands being the second step and the loss of the ligands fragments are the third or later steps with the ultimate products being the metal oxide or metal sulfide.
- (v) Generally, for copper(II) complexes there are varieties in the strength of the coordination bond formed and thermal stability depending mainly on the type of ligands used.
- (vi) In most cases the values of the kinetic parameters obtained from Horowitz-Metzger equation are higher than the values obtained from Coats-Redfern equation. This is due to the inherent error involved in the approximation method employed in the derivation of the Horowitz-Metzger equation.
- (vii) In general, there is a direct relation between  $E^\ddagger$  and  $Z$  for the obtained complexes. The relatively low values of  $Z$  indicate the slow nature of the pyrolysis reaction.
- (viii) In most cases the values of the activation energy for the second stage of decomposition were found

to be higher than that of the first stage, which indicates that the decomposition rate of the second stage is lower than the first. This may be attributed to the structural rigidity of the remaining complex<sup>[17,19,38]</sup>.

- (ix) The order  $n$  of the decomposition reactions does not provide any meaningful information about the decomposition mechanisms of the complexes<sup>[39]</sup>.

## REFERENCES

- [1] N.Eweiss, A.Bahajaj, E.Elsherbini; *J.Heterocyclic.Chem.*, **23**, 1451 (1986).
- [2] I.Awad, A.Abdel-Rahman, E.Bakite; *J.Chem.Tech.and Biotech.*, **51**, 433 (1991).
- [3] M.S.Yadawe, S.A.Patil; *Tran.Met.Chem.*, **22**, 220 (1997).
- [4] M.V.Kulkarni, V.D.Patil, V.N.Biradar, S.Nanjappa; *Arch.Pharm.*, **34**, 435 (1981).
- [5] T.Somorai, G.Szilagy, J.Reiter, E.Bozo, G.Nagy, J.Janaky; *Eur.Pat.Appl.EP 15548*, 81 (1985).
- [6] M.Ghassemzadeh, M.Tabatabaee, S.Soleimani, B.Neumuller; *Z.Anorg.Allg.Chem.*, **631**, 1871 (2005).
- [7] O.P.Pandey, S.K.Sengupta, S.C.Tripathi; *Inorg.Chim.Acta.*, **90**, 91 (1984).
- [8] S.N.Dubey, R.N.Handa, B.K.Vaid; *Monatsh.Chem.*, **125**, 395 (1994).
- [9] C.Preti, G.Tosi; *Aus.J.Chem.*, **29**, 543 (1976).
- [10] B.K.Gupta, D.S.Gupta, U.Agarwala; *Bull.Chem.Soc.Japan.*, **51**, 2724 (1978).
- [11] L.Labanauskas, V.Kalca, E.Udrenaite, P.Gaidelis, A.Brukštus, V.Daukšas; *Pharmazie*, **56**, 617 (2001).
- [12] K.Singh, M.S.Barwa, P.Tyagi; *Eur.J.Med.Chem.*, **41**, 147 (2006).
- [13] K.Singh, P.D.Singh, S.M.Barwa, P.Tyagi, Y.Mirza; *J.Enz.Inhib.Med.Chem.*, **21**, 749 (2006).
- [14] K.B.Gudasi, P.B.Maravalli, T.R.Goudar; *J.Serb.Chem.Soc.*, **70**, 643 (2005).
- [15] K.B.Gudasi, S.A.Patil, R.S.Vadavi, R.V.Shenoy, M.S.Patil; *Transition Met.Chem.*, **30**, 1014 (2005).
- [16] D.A.Naik, M.Satish, Annigeri, B.Umesh, Gangadharmath, K.V.Revankar, B.V.Mahale, K.V.Reddy; *Indian J.Chem.*, **41A**, 2046 (2002).
- [17] P.B.Maravalli, K.B.Gudasi, T.R.Goudar; *Transition Met.Chem.*, **25**, 411 (2000).
- [18] P.B.Maravalli, K.B.Gudasi, T.R.Goudar; *Indian J.Chem.*, **39A**, 1087 (2000).

- [19] P.B.Maravalli, T.R.Goudar; *Thermochim.Acta*, **325**, 35 (1999).
- [20] A.Kumar, G.Singh, R.N.Handa, S.N.Dubey; *Indian J.Chem.*, **38A**, 613 (1999).
- [21] S.Yadav, O.P.Pandey, S.K.Sengupta; *Transition Met.Chem.*, **20**, 107 (1995).
- [22] S.Goel, O.P.Pandey, S.K.Sengupta; *Thermochim.Acta*, **133**, 359 (1988).
- [23] S.N.Dubey, B.Kaushik; *Indian J.Chem.*, **24A**, 950 (1985).
- [24] A.W.Coats, J.P.Redfern; *Nature*, **20**, 68 (1964).
- [25] H.H.Horowitz, G.Metzger; *Anal.Chem.*, **35**, 1464 (1963).
- [26] S.S.Kandil, B.G.El-Hefnawy, A.E.Baker; *Thermochim.Acta*, **414**, 105 (2004).
- [27] S.A.El-Gyar, M.A.El-Gahami, A.Abd El-Sameh, S.A.Ibrahim; *Polish J.Chem.*, **81**, 1387 (2007).
- [28] A.Cansiz, M.Koparir, A.Demitdag; *Molecules*, **9**, 204 (2004).
- [29] K.C.Ragenovic, V.Dimova, V.Kakurinov, D.G.Molnar, A.Buzarovska; *Molecules*, **6**, 815 (2001).
- [30] J.R.Reid, D.Heindel; *J.Heterocyclic.Chem.*, **13**, 925 (1976).
- [31] F.B.Ali, S.W.Al-Akramawi, H.K.Al-Obaidi, H.A.Al-Karboli; *Thermochim.Acta*, **419**, 39 (2004).
- [32] A.A.Said, M.R.Hassan; *Poly.Degrad.Stab.*, **39**, 393 (1993).
- [33] M.P.Madhusudanan, M.K.K.Yusuff, R.G.C.Nair; *J.Therm.Anal.*, **8**, 31 (1975).
- [34] R.D.Dakternieks, P.D.Gradon; *Aust.J.Chem.*, **24**, 2509 (1971).
- [35] S.P.Shetty, Q.Fernando; *J.Am.Chem.Soc.*, **92**, 3964 (1970).
- [36] O.J.Hill, P.J.Murray, C.K.Patil; *Rev.Inorg.Chem.*, **363**, 14 (1994).
- [37] P.Roman, I.J.Beitia, A.Luque, G.C.Miralles; *Polyhedron*, **13**, 2311 (1994).
- [38] M.K.K.Yusuff, R.Sreekala; *Thermochim.Acta*, **159**, 357 (1990).
- [39] D.B.Brown, E.G.Walton, J.A.Dilts; *J.Chem.Soc.Dalton Trans.*, **6**, 845 (1980).